coatings

MDPI

Article

Hybrid Activity of P–Si–N Moieties for Improved Fire Retardancy of Cotton Fabric Coated Using Sol-Gel Process

Zeeshan Ur Rehman *, Hamid Hassan, Laila Khan, Lee Hwain, Yun Chiho and Bon Heun Koo *

College of Mechatronic Engineering, Changwon National University, Changwon 51140, Gyeongsangnam-do, Republic of Korea; hamidhassan774@gmail.com (H.H.); coatxp@gmail.com (L.K.)
* Correspondence: zeeshan.physics@gmail.com (Z.U.R.); bhkoo@changwon.ac.kr (B.H.K.)

Abstract: A sol-gel matrix was generated from S– and P-based acids to prepare a fire-retardant solution system for coating natural cotton fibers. The physical properties, surface morphology, and elemental composition of the coated samples were assessed using optical scanning electron microscopy. The thermal behavior of the coated samples was documented using TGA and VFT tests, which confirmed higher thermal stability of the phosphate-based coatings. High char residue formation (~44.5%) and self-extinguishing properties were observed for the phosphate-based coating under non-curing conditions. The superior properties of phosphate-based coatings P5-4h could be ascribed to the collaborative effect of P–Si–N—i.e., the combined activity during the combustion process and pyrolysis of the coated sample.

Keywords: microstructure; sol-gel; thermal properties; synergism; UL–94; fire retardant

Citation: Rehman, Z.U.; Hassan, H.; Khan, L.; Hwain, L.; Chiho, Y.; Koo, B.H. Hybrid Activity of P–Si–N Moieties for Improved Fire Retardancy of Cotton Fabric Coated Using Sol-Gel Process. *Coatings* **2024**, *14*, 1283. https://doi.org/10.3390/coatings14101283

Academic Editor: Olga A. Shilova

Received: 4 September 2024
Revised: 2 October 2024
Accepted: 5 October 2024
Published: 8 October 2024

1. Introduction

The massive use of textile fabrics enhances human life. Several distinctive characteristics, such as noble texture, comfort, excellent hygroscopicity, biodegradability, "breathability", and antistatic properties, account for the widespread use of these fabrics. However, two major deficiencies hinder widespread application in a diverse spectrum of areas, ranging from the high-tech industry to home commodities made from cotton fabric: high intrinsic flammability and ignitability, which can lead to serious property and human loss during fire accidents [1–4]. Existing commercial fire-retardant solutions in the form of Pyrovatex CP or Proban can offer a satisfactory reduction in flammability [5]. However, due to increasing restrictions of laws/regulations regarding the use of toxic fire-retardant chemicals, particularly the halogen group derivatives [6,7], and some phosphorus-based compounds, including tetrakis hydroxymethyl phosphonium chloride (THPC) and N-methylol dimethyl phosphono-propionamide (MDPA), which have the potential to release formaldehyde [8], this is highly discouraged. Therefore, eco-friendly, non-toxic chemicals or their combinations, which can fulfill demands as superior fire retardants, are highly desired. A surface modification approach has been effective for the deposition of various chemicals on cotton fabric to impart fire-retardant properties. Major surface modification can be accomplished, including; layer-by-layer deposition techniques [9–17], the application of reactive monomeric or polymeric species [18–23], coating with phosphorous-containing biomolecules such as DNA or casein [20,24,25], treatment with UV–curable [26,27] or plasma-curable systems [28], and the use of sol-gel techniques [29–33].

For several reasons, such as the capacity for trapping both organic and inorganic compounds on the surface of fabric and the simplicity of the process, interest in the use of the sol-gel process for depositing fire-retardant materials onto the surface of textile fabric has remarkably grown in the last decade. The textile field has been so responsive to the sol-gel process that it has been successfully adopted for various applications such as the production of antimicrobial and UV radiation protective materials [34–39], the generation of materials

exhibiting dye fastness, anti-wrinkle finishing, super-hydrophobicity, and immobilization of biomolecules. Furthermore, sol-gel-derived hybrid structures have shown substantial effectiveness for thermal insulation, significantly enhancing the flame retardancy of coated substrates. Especially when applied to cellulosic substrates, these inorganic structures absorb ambient heat, forming a physical barrier that protects the degrading polymer by restricting heat transfer from the combustion zone. That insulation not only reduces the generation of volatile compounds that contribute fuel to the combustion zone but also accelerates the development of a carbonaceous layer (char). Moreover, this char layer contributes to flame retardancy by providing an extra layer of thermal protection. A sol-gel coating offers an interesting combination of physio-chemical activity to impart nano-modification and nano-structuring to the fabric surface. A large alkoxide $Si(OR)_4$ may be used to form sol and gel through hydrolysis and a polycondensation process. Depending on the conditions, a hybrid organic-inorganic polymer is created with linear branches or colloid elements. Silica acquired via the sol-gel process from the precursor tetraethoxysilane (TEOS) can improve the thermal resistance of the cotton to some extent. The presence of additional moieties such as N-based and P-based units may enhance performance. This is superior to simply doping flame-retardant additives (N-, B-, and P-) into silica sol during the sol-gel process. Coatings generated using this method could face poor washing durability for treated fabrics. Therefore, there has been growing interest in utilizing alkoxysilane precursors bearing evaporative chemical moieties in this process. Extensive analysis of the individual and combined role of nitrogen, phosphorous, and silicon units in precursors has been reported [31,32,40,41]. However, the precursors used are highly complex and expensive, which limits their commercial use. Thus, the use of cost-effective precursors displaying enhanced fire retardancy is of great interest. Generally, hydrochloric acid is used to catalyze the gelation process during the sol-gel method. However, in the current study, phosphoric acid and sulfuric acids were used to achieve gelation as well as cause significant improvement in the flame extinguishing and thermal stability of the cotton fabric. The formation and effect of (P–N–Si) and (S–N–Si) cross-linkers on the FR and structural properties have been evaluated. A hybrid silica gel has been formed through the addition of two types of acids, i.e., phosphoric acid and sulfuric acid; subsequently, melamine (N-precursor) was introduced to obtain a P–Si–N-based gel for deposition as a coating on cotton fabric.

2. Experimental Section

2.1. Materials

The experimental substrate consisted of 100% pure cotton fabric (180 g m^{-2}). Prior to use, the fabric was cut precisely into sample pieces (height/width~230 mm/120 mm), followed by cleaning and drying to prepare it for experimentation. Ethanol and HCl were purchased from Sigma Aldrich Seoul, Republic of Korea, however, melamine and tetraethoxysilane (TEOS) were purchased from Samchun Republic of korea. H_2SO_4 and H_3PO_4 additives were obtained from Sigma Aldrich industry Republic of Korea, Seoul. DI water used in the experiment had a resistivity of 18.6 Ω·cm.

2.2. Preparation of Sol

The sol was prepared using the following chemical ratios: TEOS:ETHANOL:DI = 1:2:4. After thoroughly mixing these chemicals, 1 mL of HCl (37%), 5 mL of H_2SO_4, and 5 mL of H_3PO_4 were added to the mixture, and stirred at room temperature for 4 h until a clear transparent sol-gel system was achieved. Simultaneously, a 10% melamine solution was prepared using ethanol and subsequently blended with the sol during the stirring process. The resulting sol was then transferred into a 500 mL beaker for cotton impregnation.

2.3. Cotton Treatment

A total of 8 sequential cotton fabric samples, each measuring 230 mm × 120 mm, were taken for the treatment. Under each experimental condition, two fabric samples were

treated. Samples P5-4h-C and P5-4h were treated in the phosphoric acid-based solution under the conditions mentioned in Table 1. Likewise, S3-4h-C and S5-4h were treated in the sulfuric acid-based sol-gel system under the conditions mentioned in Table 1. The letter "C" with the sample abbreviation was used for the curing process.

Table 1. Experimental parameters and adds on (%).

Samples	Dipping Time (hrs)	Weight before Coating (g)	Weight after Coating (g)	Adds on (%)	Heating Time/T	Curing Time/T
S5-4h	4	3.46	4.97	30.30	12 h/65 °C	60 s/130 °C
S5-4h-C	4	3.49	5.14	32.11	12 h/65 °C	60 s/130 °C
P5-4h	4	3.50	5.13	31.74	12 h/65 °C	60 s/130 °C
P5-4h-C	4	3.39	4.97	31.84	12 h/65 °C	60 s/130 °C

2.4. Characterization Techniques

By using a low–voltage scanning electronic microscope (LV-SEM, Merlin Compact), examined the surface morphologies of both treated and untreated fabric species. Additionally, to investigate the elemental composition of coated surfaces, EDAX (energy-dispersive X-ray spectroscopy) was used as a combined means of characterization alongside LV-SEM. To enhance surface microscopy effectiveness, the as-coated fabric samples were Pt-sputtered for 3 min under high vacuum conditions to facilitate conduction to the fabric surface. To quantitatively evaluate the attachment of coating species to the cotton fabric, pre- and post-coating weight was measured using a highly sensitive weight balance (5 digits). The coated samples were then analyzed using attenuated total reflection Fourier transform infrared (ATR-FTIR) spectroscopy (JASCO 6300) over a frequency range of 4000 to 400 cm^{-1}. The spectra profiles were collected after 32 scans at a resolution of 4 cm^{-1}. Additionally, the thermal stability of both uncoated and coated fabrics was then assessed in a nitrogen atmosphere (20 mL min^{-1}) using the Sinco Thermogravimetric Analyzer (N-1000/1500) within the temperature range of 50–700 °C, with a heating rate of 20 °C min^{-1}. Each sample, weighing 10~15 mg was placed in an empty Pt crucible, which was then balanced with a standard one before being introduced into the heating chamber. Macro-combustion tests, including the vertical flame test (VFT), were conducted for both the coated and the control samples in accordance with documented ASTM D6413 standards. Accordingly, each sample was ignited in a lab-manufactured vertical flammability chamber (300 mm/120 mm) using a Bunsen burner flame. The flame was directed to the fabric sample for precisely 10 s, positioned 20 mm below it, and the entire process was captured using a high-speed optical camera.

3. Results and Discussion

3.1. Microstructural and Physical Properties

Optical images of the samples of treated cotton fabric obtained in different additives and concentration conditions were taken and analyzed for rupture tests as shown in Figure 1. All the processing conditions applied for the coating formulation process and subsequent post-coating treatment conditions can be seen in Table 1. Images show no significant apparent changes, except the intrinsic physical properties of the coated cotton. It can be seen that except P5-4h, all the samples, including the sulfur-based coated and phosphorus-based coated samples, were ruptured. This suggests the combined effect of chemical and heat processes on the mechanical properties of the coated samples. P5-4h sustained the maximum possible force in order to resist the rupturing process. Importantly, it can be seen that the rupture line is very straight and sharp, suggesting the brittleness of the fabric in the cases of S5-4h-C and P5-4h-C. However, in the case of S5-4h, the rupture line is not sharp instead, fibers mesh alongside can be seen evidently, which suggests a lower degree rupture process in the S5-4h. Since there is a possibility that the heating procedure could induce a reaction between the acidic component and silica network to

react and potentially activate an exothermic reaction in the presence of a high-temperature environment. This reaction could lead to damage in the cellulosic network of the cotton fabric, as can be observed in the first two samples. Further, from the sharp and straight rupture line in S5-4h-C and P5-4h-C samples, it can be presumed that the curing process aggravated the rupturing and thus significantly compromised the mechanical properties of the coated samples. Add-on's % was calculated from the weight comparison between the coated and uncoated samples using the following equation and was drawn as shown in Figure 2.

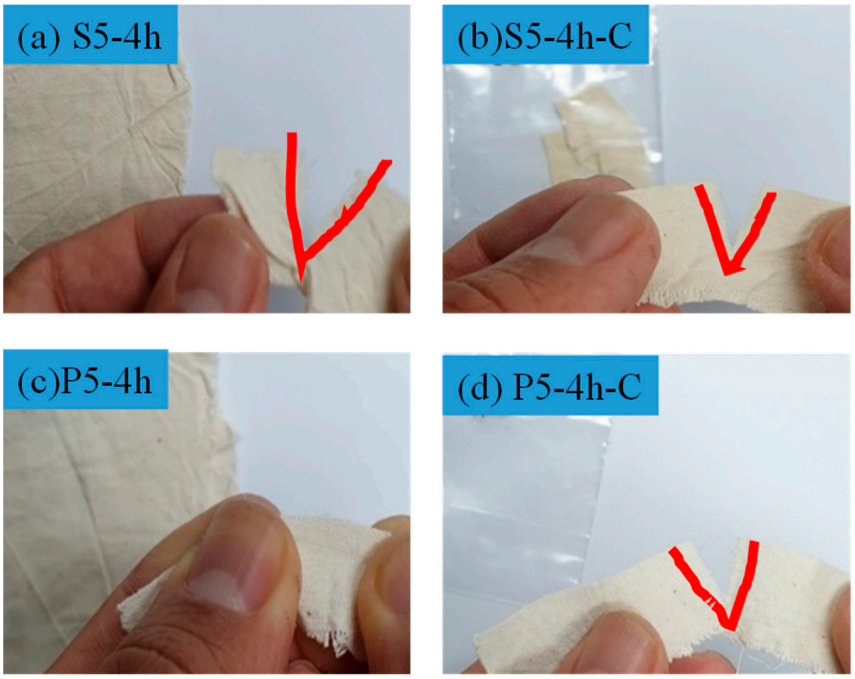

Figure 1. (**a**–**d**) Optical images of the coated cotton samples showing rupturing performance indicated by red lines.

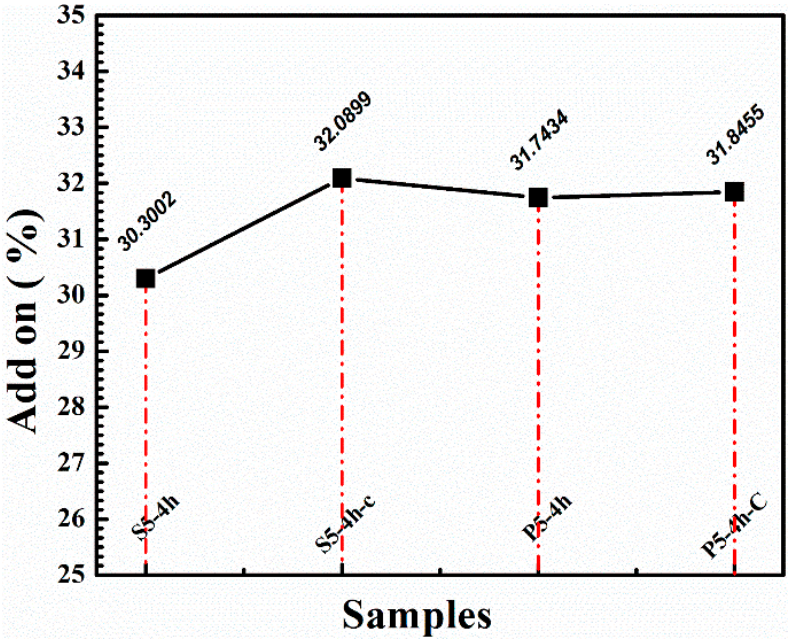

Figure 2. Add-on's (%) of the coated species obtained from the weight difference before and after coating for each sample.

$$W_{add-on}(\%) = \frac{W_2 - W_1}{W_1} \times 100$$

Here W_1 represents the weight of the untreated fabric and W_2 is the weight of the treated fabric. It can be seen that more than 30% of the coated material was deposited on the cotton fabric. In the case of P5-4h-C and P5-4h, the weight gain is higher compared to the sulfur-based coated sample (S5-4h).

The treated cotton samples were subsequently analyzed using a low–voltage scanning electron microscope, which allows an understanding of the coating process and its effect on the fabric's microstructure as shown in Figure 3a–d. We can observe the results, which provided valuable insights into the deposition of coating layers at a micro-level scale. The SEM images of the treated fabric samples demonstrated a surface that appears consistently smooth, with clearly visible gaps between the fibers. Furthermore, a denser and more cohesive coating is observed on the surfaces of the coated samples. It can be seen in Figure 3 that the fiber thickness is increased after treatment, which suggests that the coating deposited successfully, and also, uniform coverage of all the fibers on the fabric by the coated layers can be observed. This uniformity suggests a controlled application process and enhancement across the entire fabric surface. Such precision in coating application signifies a sophisticated manufacturing technique aimed at enhancing the fabric's properties while maintaining its integrity. Further, the original microstructure of the fabric can be seen as clear and distinctive, without any ceiling or tapping by thick sheet layers of the coated species. The coated species, however, sealed the individual fibers of the cotton fabric instead of covering the entire fabric matrix. Coating of the individual fibers suggests the perseverance of the originality of the fabric microstructure. Unlikely, the coating layers on the P5-4h-C can be seen as thick and seal the cotton fabric microstructure at various random locations. Thus, the individual fibers of the cotton fabric cannot be resolved as compared to other samples. Similarly, from the high-resolution images of the P5-4h-C, the coating layers can be seen as broken into patches, which validates the higher thickness of the coating layers as compared to other samples. Furthermore, micro-details can be observed from the individual fiber images as shown in the high-resolution (HR) images of the respective samples. The HR images present the level of thickness of coating layers and fabric matrix.

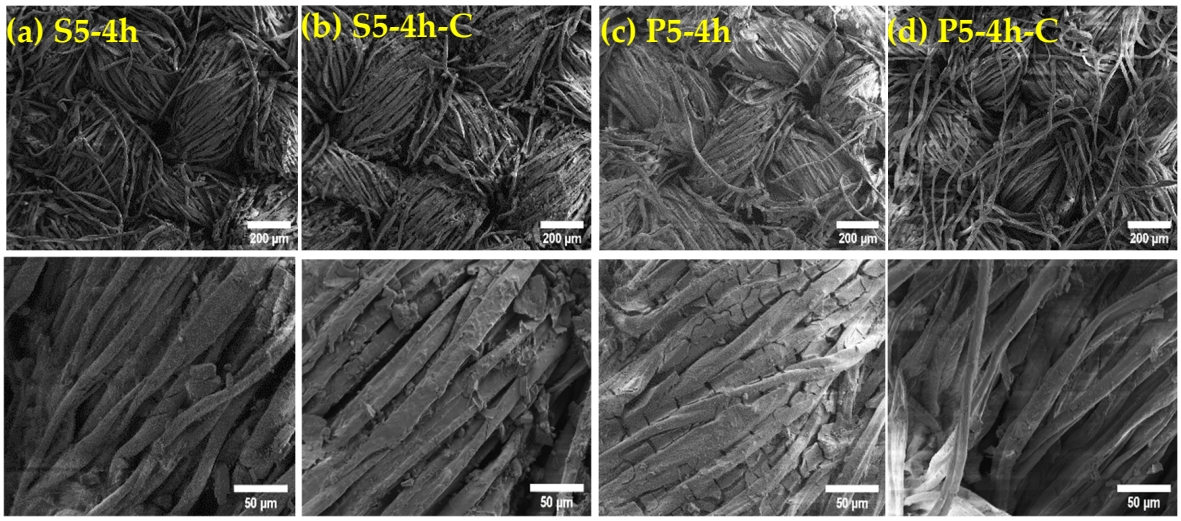

Figure 3. (**a**–**d**) LV-SEM images of the coated samples obtained under various conditions.

3.2. Compositional Analysis

Elemental compositional profiles of the samples were obtained via EDS mapping of the whole sample as shown in Figure 4 and numerically recorded in Table 2. Generally, C, O, Si, P, S, and N were obtained in the elemental profiles. Importantly, % of "Si" was found higher in the sulfur-based samples at ~6.25 and ~8.37 compared to phosphate-based

samples at ~5.90 and ~4.23. The Si was majorly obtained from the TEOS, a sol-gel precursor. The presence of a significant amount of "Si" indicates the successful deposition of the sol-gel species to the individual fiber, and consequently, it could aid in safeguarding the coated fabric against fire. The acid species that were added were also obtained in the EDS spectra with numerical values above 2% for both phosphorous and sulfur. The presence of sulfur and phosphorous suggests effective hydrolysis and condensation during the sol-gel deposition process and thus successful deposition of coatings.

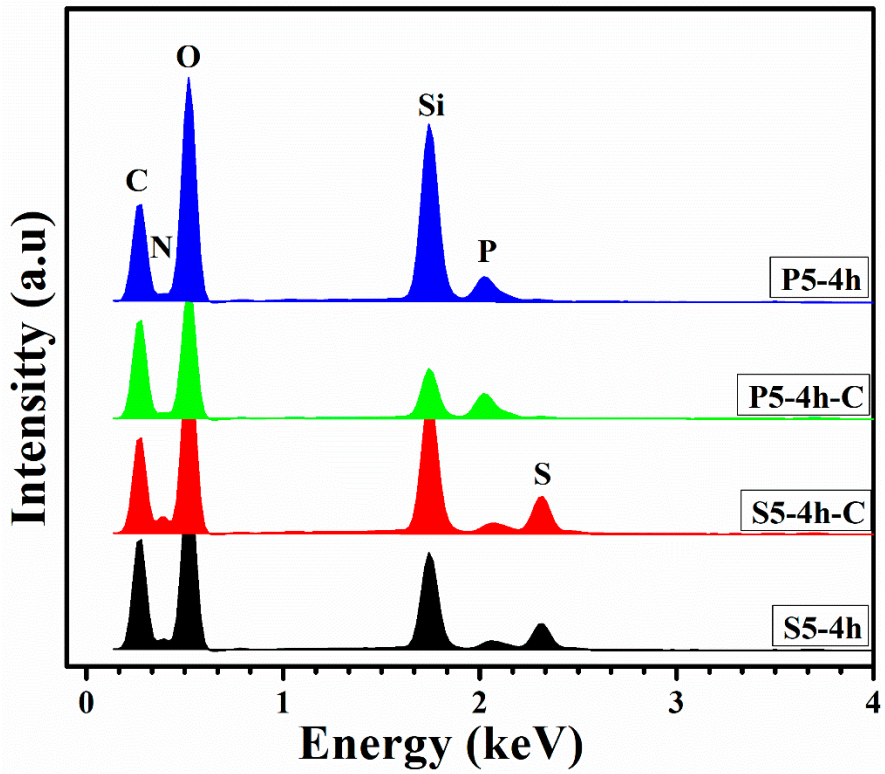

Figure 4. EDS profile of the coated fabric samples.

Table 2. EDS compositional profile of the coated samples.

Elements#	S5-4h	S5-4h-C	P5-4h	P5-4h-C
C	44.63	41.79	46.72	46.78
P			1.38	2.11
O	46.62	46.37	45.91	46.67
Si	6.25	8.37	5.90	4.23
S	2.36	3.26	-----	-----
N	0.14	0.21	0.09	0.21
Total	100.00	100.00	100.00	100.00

FTIR analysis of the coated samples was carried out, and the results are plotted as shown in Figure 5. The peaks observed in the coated samples correspond to various stretching and vibrational modes associated with the bonds between the coating species deposited on the cotton fabric. The major modes as identified in the cotton fabric include OH stretching, CH stretching, H_2O absorption, CH absorption, CH_2 bending, C-O-O glycoside bend stretching, and C-H rock vibration. The OH and CH stretching were observed at wave numbers exceeding 2500 cm^{-1}, exhibiting lower energy levels for these resonances. It is hypothesized that these vibrations have stemmed from the presence of C-H and O-H groups in both the ethanol and cotton fabric. Moreover, it is observable that the width of these two peaks has been significantly modified under different coating conditions, indicating that OH groups may be removed through an extended heating duration.

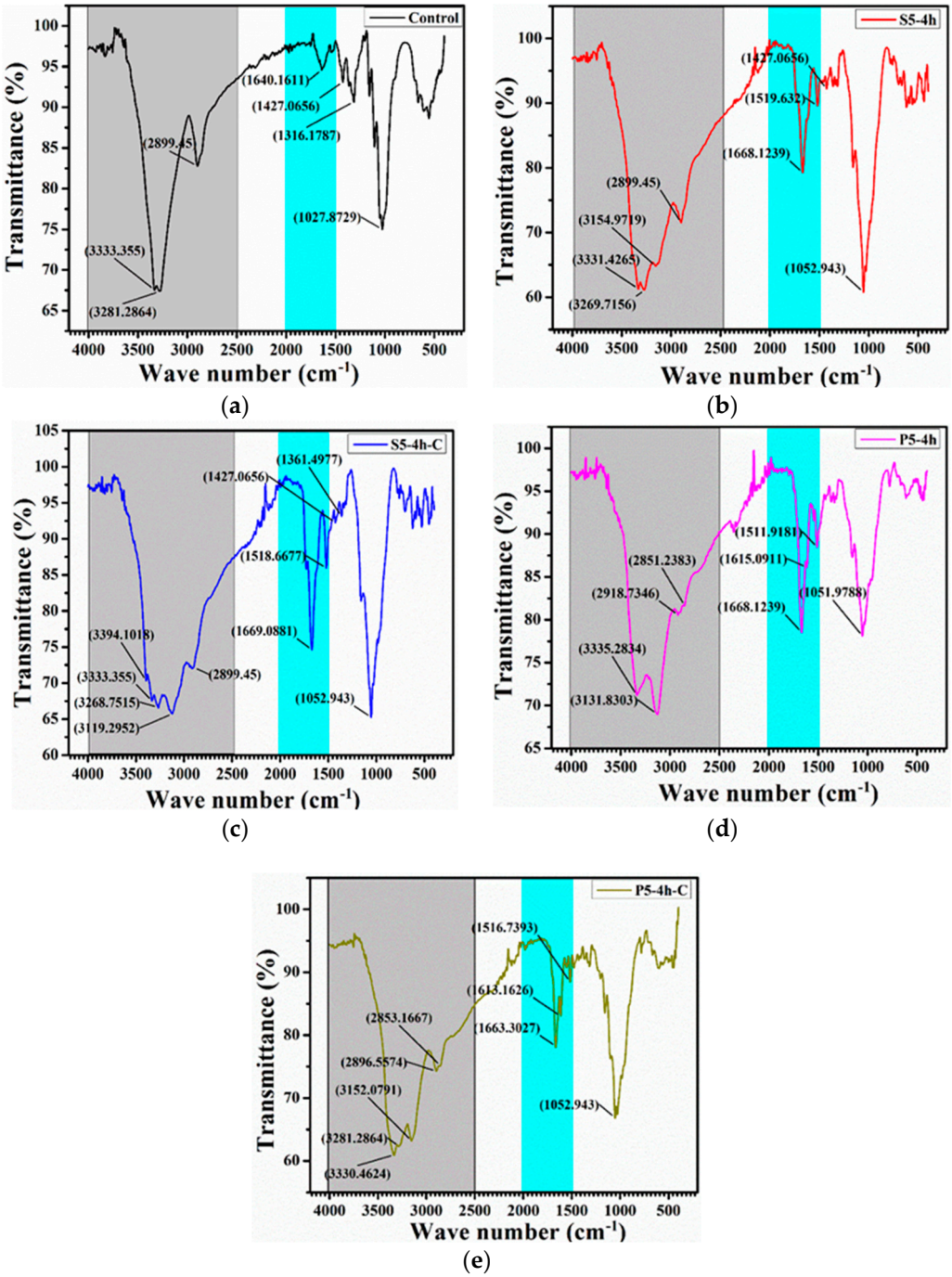

Figure 5. (**a**–**e**) FTIR analysis profile of the coated cotton fabrics.

The hydrolysis of the Si–OR group as it proceeded through the sol-gel process could possibly decrease the intensity of the absorption peaks of C–H groups belonging to the alkoxy groups at approximately 2900 cm^{-1} [42]. However, the degree of decrease varies with the type of additives, suggesting the efficiency of the sol-gel process. It can be seen that the decrease in C–H peaks was higher for P5-4h-C and P5-4h, suggesting improved hydrolysis and sol-gel processes. The formation of the Si–OH groups results in an increased intensity of the absorption peak of −OH groups around 3450 cm^{-1} [43,44]. Additionally, the formation of Si–O–Si and/or Si–O–P networks can cause the absorption peaks to broaden around ~1150 cm^{-1} [43]. Furthermore, the phosphate units exhibit four principal domains in the IR spectrum, each corresponding to specific vibration modes: the symmetric stretching mode (νs) from 900 to 1000 cm^{-1}, the antisymmetric stretching mode (νas)

between 1000 and 1250 cm^{-1}, the antisymmetric bending mode (δas) from 500 to 700 cm^{-1}, and the symmetric bending mode (δs) between 300 and 500 cm^{-1}. In the studied compound, the bands identified between 1010 and 1185 cm^{-1} correspond to the triply degenerate νas (PO_4) mode, while the band near 962 cm^{-1} is attributed to the νs (PO_4) mode in the stretching vibration domain. For the bending modes, bands were assigned to the doubly degenerate δs (PO_4) (ranging from 383 to 461 cm^{-1}) and the triply degenerate δas (PO_4) modes (ranging from 492 to 628 cm^{-1})

3.3. Thermal Analysis

To examine the thermal degradation stability, deterioration stages, and ash residue of the treated cotton, thermogravimetric analysis was performed for all the treated species. TGA was conducted over a temperature range of 25 °C to 700 °C at a heating rate of 20°/min as shown in Figure 6, and the obtained parameters were recorded as in Table 3. T_{on} (onset temperature, where the degradation starts) and T_{off} (offset temperature, where the degradation ends) for each sample can be seen in Table 3. P-based samples have a higher T_{on} and a lower T_{off}, suggesting a limiting region of degradation. It can be seen that the rapid degradation that occurred between 320 °C and 460 °C was due to the thermal degradation of the polymer backbone through pyrolysis. It is significant to mention that the char yield obtained for phosphorous-based samples was above ~40%. The highest value of residue was obtained for P5-4h ~44.5, followed by P5-4h-C ~41.99%. At higher temperatures (350~500 °C), phosphoric acid is converted into pyro-meta and poly-phosphate species, as illustrated in Figure 6b. The reaction route through which the formation of these species occurred is presented in Equation (1). These phosphate species, which were also identified in the FTIR profile, at higher temperatures could form a strong shield on the outermost layer of the cotton fabric, thereby delaying the further decomposition of the material, while the latter could have an additional effect of diluting the oxidizing gaseous species [44].

Table 3. Parameters obtained from the thermal analysis of the coated samples.

#	T_{on}	R_{on}	T_{off}	R_{off}	T_{peak1}	T_{peak2}	Char Residue (%)
S5-4h	155.27	92.44	340.53	53.1	232.61	297.18	34.0
S5-4h-C	146.77	95.82	355.45	56.24	226.26	281.75	40.81
P5-4h	227.60	92.37	281.99	68.03	145.5		44.5
P5-4h-C	229.87	92.59	284.07	65.84	283.87		41.99

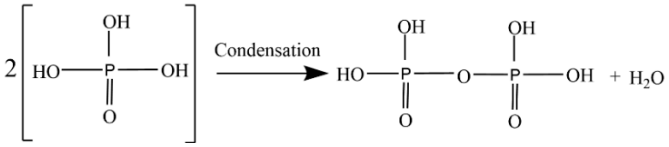

(1)

It has been reported that phosphorous agents significantly boost the char yield [45]. Furthermore, phosphoric acid showed a catalytic role in the dehydration reaction of terminal alcohols as shown in Equations (1)–(4), represented by the endothermic plateau on the TGA plot. Such dehydration at lower temperatures results in the generation of carbocations and unsaturated carbon species, which convert to stable carbonized structures at higher temperatures.

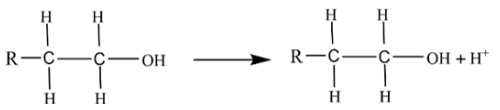

(2)

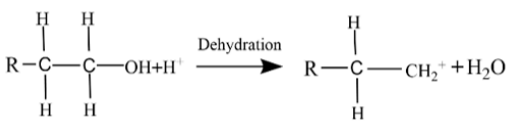

(3)

(4)

Furthermore, several other significant effects of these carbonized layers were observed, such as (a) limiting the volatilization of fuel, (b) limiting the oxygen diffusion to the cotton matrix, and (c) insulating the cotton from the surface heat. In addition, the formation of poly-phosphoric acids and pyrophosphate allows the silicon reaction during pyrolysis to convert into silicate and form a protective layer, which further retards the thermo-oxidative combustion of cellulose [45–47]. It is also believed that phosphoric acid can produce active radicals (PO_2^-, PO^-, HPO^-), which act as scavengers of H^+ and OH^-, thus inhibiting the combustion process 10 times more effectively than chlorine during pyrolysis [48]. The melamine (N-Source) is used as an additive to catalyze the production of char and thus co-inhibit the pyrolysis process in combination with P-Si. Therefore, the use of a sole precursor, e.g., silicon, can also be responsible for the higher residue [49–51]. The combination of the Si-P-N network offered significant thermal resistance against fire and higher char residue as observed for P5-4h and P5-4h-C samples. It is also believed that the Nitrogen species produced during the degradation process could lead to the formation of gaseous phosphaphenanthrene groups in the presence of acidic phosphorus groups. Likewise, the phosphaphenanthrene groups further combine with silicon groups to promote the char formation. On the contrary, char residue obtained for the S5-4h and S-4h-C were found to be significantly lower at 38.8 and 34%, respectively, as shown in Figure 6. The sulfur species could not collaborate with "Si" and "N" to form a networking effect against the combustion and pyrolysis processes.

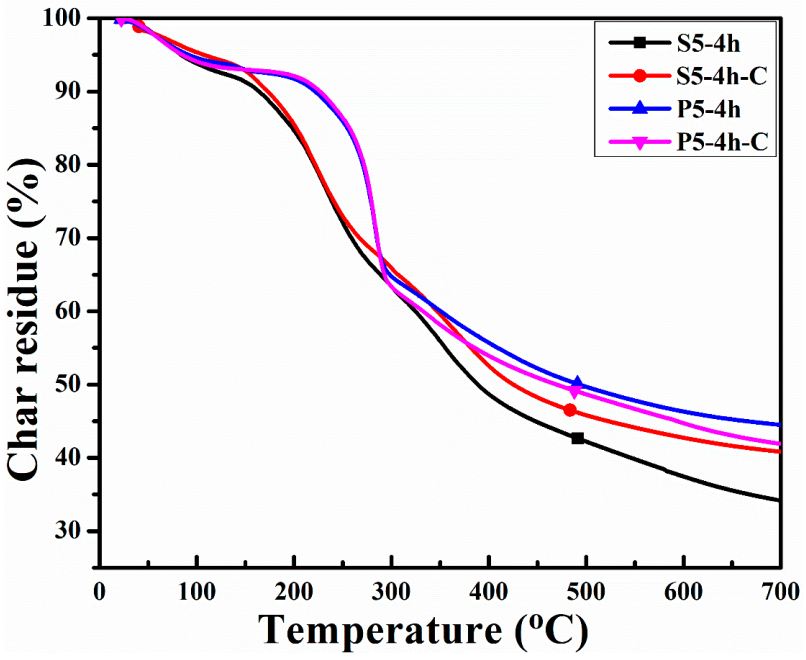

(**a**)

Figure 6. *Cont.*

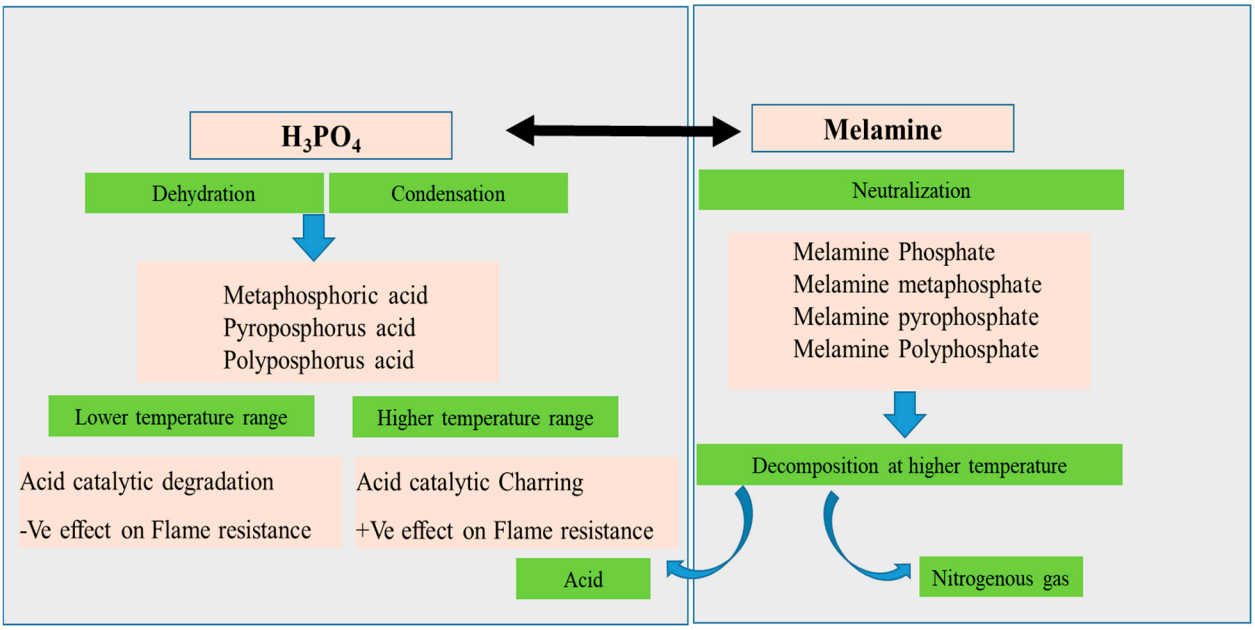

(**b**)

Figure 6. (**a**) Thermogravimetric analysis curves of the coated fabric and (**b**) reaction mechanism of the coating components during the thermal process.

The DTGA profile was obtained from the differentiation of the TGA curve to analyze the maxima and minima on the temperature axis as shown in Figure 7. The width and length of the DTGA peaks represent the temperature region and the quantity of the weight loss, respectively. The minima and maxima on the temperature axis could provide the details and identify the temperature point, where the highest and lowest degradation of the samples occurred during the thermogravimetric analysis. Endothermic peaks with different lengths for each sample appeared, as can be seen in Figure 7. The DTGA profile plot clearly shows degradation at three different temperature points. The initial degradation took place in the range of 100 °C to 150 °C, which can be attributed to the low melting point species and volatiles and is more evident in the P5-4h compared to other samples. The next degradation, which is the major degradation, occurred in the range of 200 °C to 300 °C, which is due to the pyrolysis of the cotton fabric. The major loss is much steeper but narrower for P5-4h and P5-4h-C samples compared to the S-5 sample, suggesting singular deep degradation in the P5-4h and P5-4h-C samples, albeit with less weight loss. In contrast, in S5-4h and S5-4h-C samples, the degradation occurred less steeply but extended through the wide region of the curve. Furthermore, additional degradation peaks can also be seen for S5-4h and S5-4h-C, suggesting two additional doses of weight loss for the stated samples. This could be possible due to the weak protective layers and carbonaceous structure formed during the major degradation process. As stated earlier, the carbonaceous char formed by the P–Si–N network, as in the case of P5-4h and P5-4h-C samples, has considerable retardance against fire.

For the additional examination of the thermal characteristics of the treated samples, a vertical flame test was performed, and the relevant images were captured after the removal of flame burner at intervals of 10 s, 20 s, and final char images. As shown in Figure 8, the sulfur-based samples S5-4h and S5-4h-C are easy to ignite and could not withstand the flame. The final visual representation of the stated samples is observable as fully burned, as well as mechanically disintegrated, suggesting the complete failure of the sulfur-based coatings to protect the samples against fire and subsequently against mechanical disintegration. Similarly, the char residue obtained through VFT was found to be more than 50%, which is higher than the TGA values, having erroneous inclusion, which can be attributed to the irregular burnt area. Likewise, poor values for the burning spread and

burning time were obtained for S5-4h and S5-4h-C samples as mentioned in Table 4 and plotted in Figure 9. In contrast, the phosphate-based coated samples offered significant resistance to the fire, as can be seen in Figure 8c,d. After the removal of the burning burner, the fire was immediately extinguished for both P5-4h and P5-4h-C samples, which is a significant achievement for the current combination of used materials and process. In consensus regarding the TGA results, it is observable that flame spread is higher for the P5-4h-C sample compared to the uncured sample (P5-4h) suggesting the superior role of the latter. It is believed that the curing process could cause the volatile species and lower melting point radicals to release from the cotton surface and thus could not play its role during the higher temperature tests (TGA and VFT).

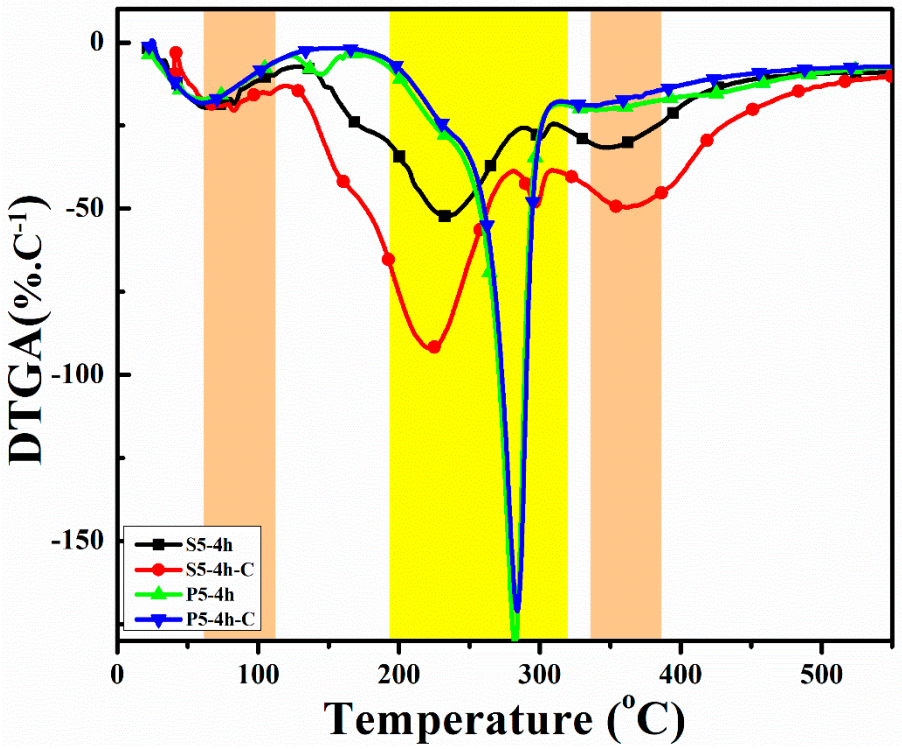

Figure 7. DTGA analysis curves of the coated fabrics obtained under various conditions.

Table 4. Combustion parameters obtained through VFT analysis.

Samples	Flame Spread (mm^2/s)	Char Residue (%)	Burning Rate (g/s)	Burning Time (s)
S5-4h	7.44	44.06	0.12	25
S5-4h-C	7.71	51.40	0.16	26
P5-4h	Fire Extinguishes			
P5-4h-C	Fire Extinguishes			

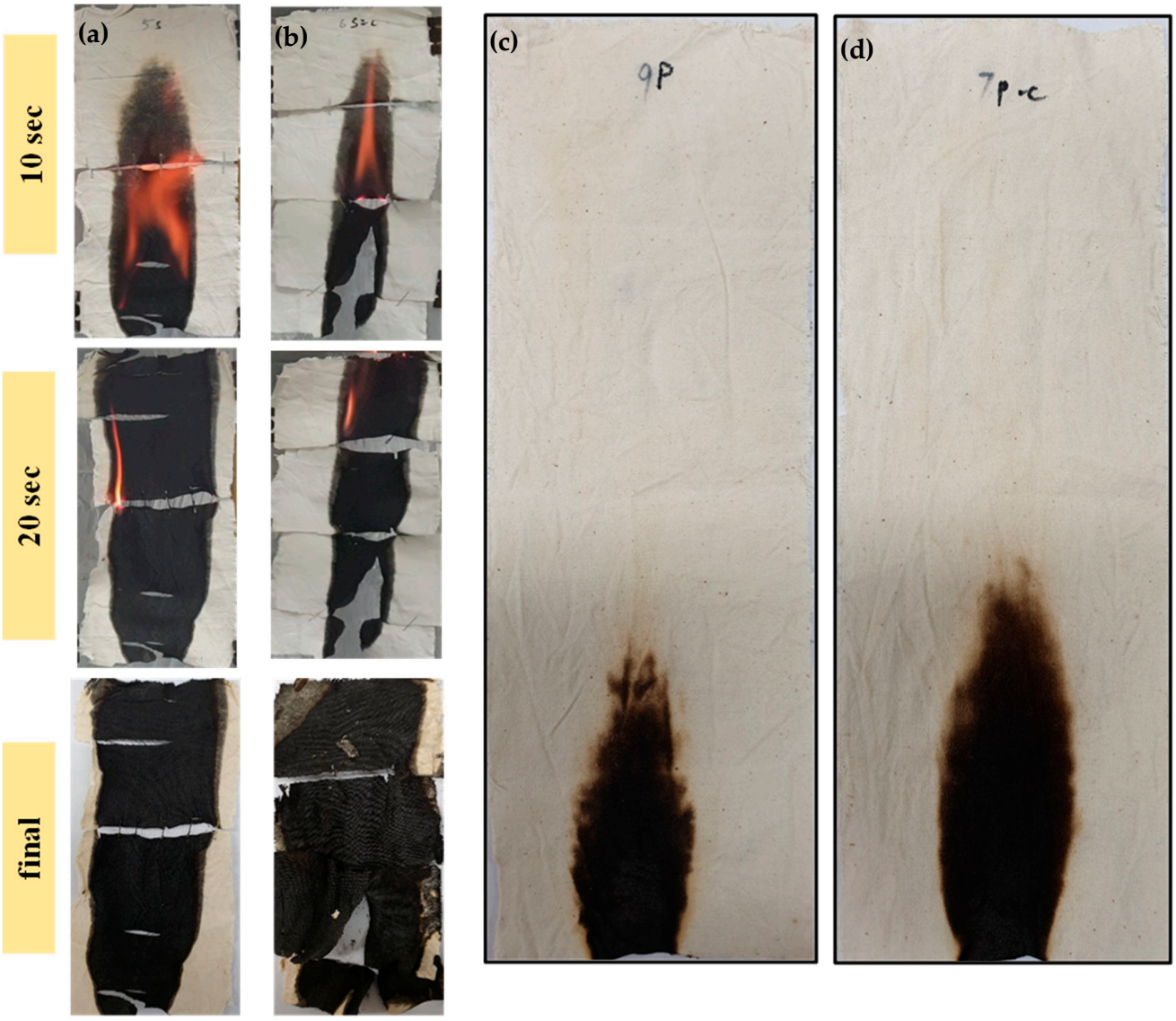

Figure 8. VFT images and flame spread after 10 s, 20 s, and final char, (**a**,**b**) sulphate based coated samples, (**c**,**d**) phosphates based coated samples. Self-extinguishing occurred in (**c**,**d**).

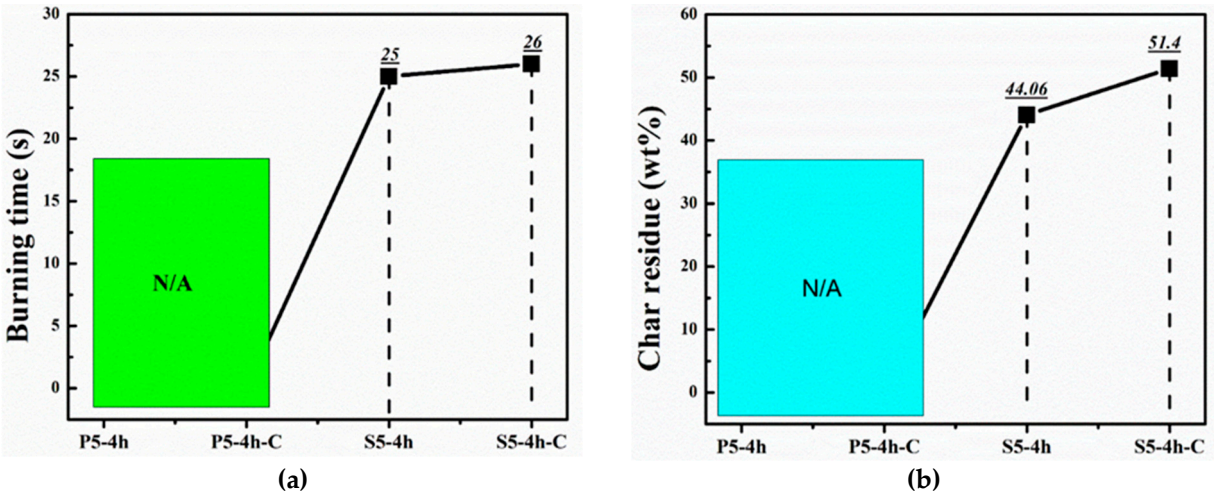

Figure 9. *Cont.*

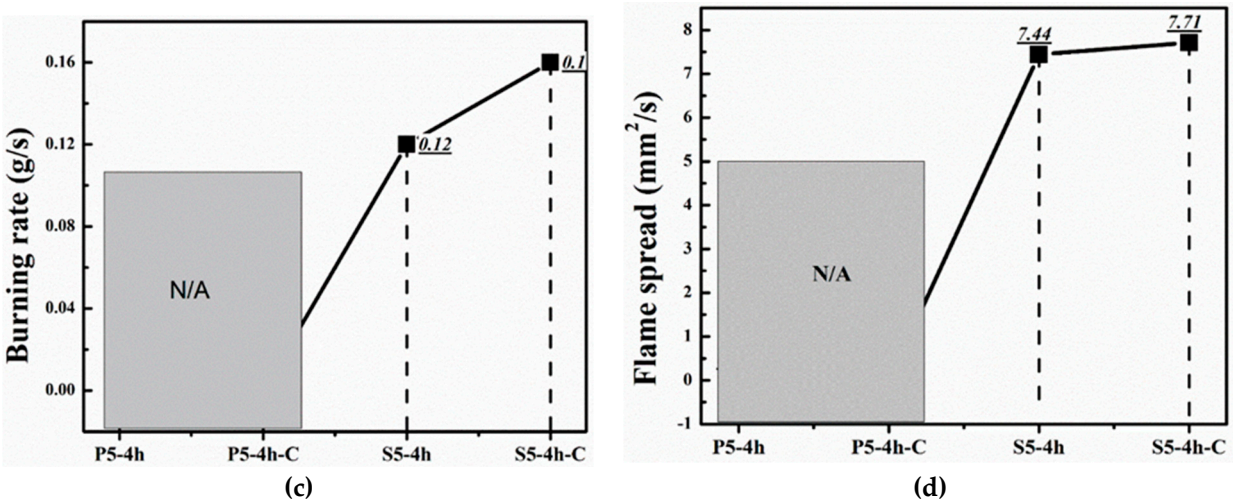

Figure 9. (**a**–**d**) Burning time, char residue, burning rate, and flame spread of the coated samples obtained from VFT data.

3.4. Conclusions

Sol-gel-based fire-retardant coatings were effectively applied onto the cotton fabric using phosphoric and sulfuric acid additives. The addition of sulfuric acid species was a complete failure due to the mechanical disintegration of the coated samples and weak fire resistance properties. On the contrary, it was found that the phosphate-based coatings offered significant protection to the cotton fabric against flame and ignition. For instance, the highest char residue was obtained for Ph-4h ~44.5%, with a peak degradation temperature of 284 °C. In addition, complete self-extinguishing occurred for both P5-4h and P5-4h-C samples, suggesting the superior protection properties of the phosphate-based coatings against ignition. The superior fire-retardant behaviors of the phosphate-based coated samples were due to the synergistic effect of phosphorus–silicon–nitrogen, i.e., the combined reaction activity during the combustion and ignition process.

Author Contributions: Conceptualization, Z.U.R., L.K., L.H., Y.C. and B.H.K.; methodology, Z.U.R., L.K. and B.H.K.; software, Z.U.R., H.H. and L.K.; validation, Z.U.R., L.K. and B.H.K.; formal analysis, Z.U.R., L.K. and B.H.K.; investigation, Z.U.R., H.H., L.K. and B.H.K.; resources, Z.U.R., L.K. and B.H.K.; data curation, Z.U.R., H.H., L.K., L.H., Y.C. and B.H.K.; writing—original draft preparation, Z.U.R. and L.K.; writing—review and editing, Z.U.R. and L.K.; visualization, Z.U.R., L.K., L.H., Y.C. and B.H.K.; supervision, Z.U.R., L.K. and B.H.K.; project administration, Z.U.R., L.K. and B.H.K.; funding acquisition, Z.U.R. and B.H.K. All authors have read and agreed to the published version of the manuscript.

Funding: The research is funded by the Education Ministry through grants from the Korea National Research Foundation (2018R1A6A1A03024509). Additionally, support is provided by the Korea Institute of Energy Technology Evaluation and Planning (KETEP) through Korean government funding (MOTIE) (20214000000480, Development of R&D engineers for combined cycle power plant technologies). Following are the results of a study on the "Leaders in Industry-University Cooperation 3.0" Project, sponsored by the Ministry of Education and National Research Foundation of Korea.

Institutional Review Board Statement: Not applicable.

Informed Consent Statement: Not applicable.

Data Availability Statement: The research data is the sole property of the university.

Conflicts of Interest: The authors declare no conflicts of interest.

References

1. Lu, S.-Y.; Hamerton, I. Recent developments in the chemistry of halogen-free flame retardant polymers. *Prog. Polym. Sci.* **2002**, *27*, 1661–1712. [CrossRef]
2. Horrocks, A.R. Flame-retardant Finishing of Textiles. *Rev. Prog. Color. Relat. Top.* **1986**, *16*, 62–101. [CrossRef]
3. Nabil, B.; Ahmida, E.A.; Christine, C.; Julien, V.; Abdelkrim, A. Polyfunctional cotton fabrics with catalytic activity and antibacterial capacity. *Chem. Eng. J.* **2018**, *351*, 328–339. [CrossRef]
4. Wang, W.; Wang, J.; Wang, X.; Wang, S.; Liu, X.; Qi, P.; Li, H.; Sun, J.; Tang, W.; Zhang, S.; et al. Improving flame retardancy and self-cleaning performance of cotton fabric via a coating of in-situ growing layered double hydroxides (LDHs) on polydopamine. *Prog. Org. Coat.* **2020**, *149*, 105930. [CrossRef]
5. Horrocks, A.R. Flame retardant challenges for textiles and fibres: New chemistry versus innovatory solutions. *Polym. Degrad. Stab.* **2011**, *96*, 377–392. [CrossRef]
6. Birnbaum, L.S.; Staskal, D.F. Brominated flame retardants: Cause for concern? *Environ. Health Perspect.* **2004**, *112*, 9–17. [CrossRef]
7. de Wit, C.A. An overview of brominated flame retardants in the environment. *Chemosphere* **2002**, *46*, 583–624. [CrossRef]
8. Horrocks, A.R. Flame retardant finishes and finishing. *Text. Finish.* **2003**, *2*, 214–250.
9. Li, Y.-C.; Schulz, J.; Mannen, S.; Delhom, C.; Condon, B.; Chang, S.; Zammarano, M.; Grunlan, J.C. Flame Retardant Behavior of Polyelectrolyte−Clay Thin Film Assemblies on Cotton Fabric. *ACS Nano* **2010**, *4*, 3325–3337. [CrossRef]
10. Li, Y.-C.; Mannen, S.; Morgan, A.B.; Chang, S.; Yang, Y.-H.; Condon, B.; Grunlan, J.C. Intumescent All-Polymer Multilayer Nanocoating Capable of Extinguishing Flame on Fabric. *Adv. Mater.* **2011**, *23*, 3926–3931. [CrossRef]
11. Chang, S.; Slopek, R.P.; Condon, B.; Grunlan, J.C. Surface Coating for Flame-Retardant Behavior of Cotton Fabric Using a Continuous Layer-by-Layer Process. *Ind. Eng. Chem. Res.* **2014**, *53*, 3805–3812. [CrossRef]
12. Carosio, F.; Di Blasio, A.; Alongi, J.; Malucelli, G. Green DNA-based flame retardant coatings assembled through Layer by Layer. *Polymer* **2013**, *54*, 5148–5153. [CrossRef]
13. Rehman, Z.U.; Niaz, A.K.; Song, J.-I.; Koo, B.H. Excellent Fire Retardant Properties of CNF/VMT Based LBL Coatings Deposited on Polypropylene and Wood-Ply. *Polymers* **2021**, *13*, 303. [CrossRef]
14. Song, K.; Hou, B.; Ur Rehman, Z.; Pan, Y.-T.; He, J.; Wang, D.-Y.; Yang, R. "Sloughing" of metal-organic framework retaining nanodots via step-by-step carving and its flame-retardant effect in epoxy resin. *Chem. Eng. J.* **2022**, *448*, 137666. [CrossRef]
15. Hou, B.; Song, K.; Ur Rehman, Z.; Song, T.; Lin, T.; Zhang, W.; Pan, Y.-T.; Yang, R. Precise Control of a Yolk-Double Shell Metal–Organic Framework-Based Nanostructure Provides Enhanced Fire Safety for Epoxy Nanocomposites. *ACS Appl. Mater. Interfaces* **2022**, *14*, 14805–14816. [CrossRef]
16. Ur Rehman, Z.; Kaseem, M.; Churchill, D.G.; Pan, Y.-T.; Heun Koo, B. Macro and micro thermal investigation of nanoarchitectonics-based coatings on cotton fabric using new quaternized starch. *RSC Adv.* **2022**, *12*, 2888–2900. [CrossRef]
17. Ur Rehman, Z.; Huh, S.-H.; Ullah, Z.; Pan, Y.-T.; Churchill, D.G.; Koo, B.H. LBL generated fire retardant nanocomposites on cotton fabric using cationized starch-clay-nanoparticles matrix. *Carbohydr. Polym.* **2021**, *274*, 118626. [CrossRef] [PubMed]
18. Yang, C.Q.; Wu, W. Combination of a hydroxy-functional organophosphorus oligomer and a multifunctional carboxylic acid as a flame retardant finishing system for cotton: Part I. The chemical reactions. *Fire Mater.* **2003**, *27*, 223–237. [CrossRef]
19. Wu, W.; Yang, C.Q. Comparison of different reactive organophosphorus flame retardant agents for cotton: Part I. The bonding of the flame retardant agents to cotton. *Polym. Degrad. Stab.* **2006**, *91*, 2541–2548. [CrossRef]
20. Yang, C.Q.; He, Q. Applications of micro-scale combustion calorimetry to the studies of cotton and nylon fabrics treated with organophosphorus flame retardants. *J. Anal. Appl. Pyrolysis* **2011**, *91*, 125–133. [CrossRef]
21. Chang, S.; Sachinvala, N.D.; Sawhney, P.; Parikh, D.V.; Jarrett, W.; Grimm, C. Epoxy phosphonate crosslinkers for providing flame resistance to cotton textiles. *Polym. Adv. Technol.* **2007**, *18*, 611–619. [CrossRef]
22. Shi, Y.; Nie, C.; Jiang, S.; Wang, H.; Feng, Y.; Gao, J.; Tang, L.; Song, P. Tunable construction of fire safe and mechanically strong hierarchical composites towards electromagnetic interference shielding. *J. Colloid Interface Sci.* **2023**, *652*, 1554–1567. [CrossRef] [PubMed]
23. Shi, Y.; Liu, C.; Duan, Z.; Yu, B.; Liu, M.; Song, P. Interface engineering of MXene towards super-tough and strong polymer nanocomposites with high ductility and excellent fire safety. *Chem. Eng. J.* **2020**, *399*, 125829. [CrossRef]
24. Alongi, J.; Milnes, J.; Malucelli, G.; Bourbigot, S.; Kandola, B. Thermal degradation of DNA-treated cotton fabrics under different heating conditions. *J. Anal. Appl. Pyrolysis* **2014**, *108*, 212–221. [CrossRef]
25. Carosio, F.; Di Blasio, A.; Cuttica, F.; Alongi, J.; Malucelli, G. Flame Retardancy of Polyester and Polyester–Cotton Blends Treated with Caseins. *Ind. Eng. Chem. Res.* **2014**, *53*, 3917–3923. [CrossRef]
26. Xing, W.; Jie, G.; Song, L.; Hu, S.; Lv, X.; Wang, X.; Hu, Y. Flame retardancy and thermal degradation of cotton textiles based on UV-curable flame retardant coatings. *Thermochim. Acta* **2011**, *513*, 75–82. [CrossRef]
27. Opwis, K.; Wego, A.; Bahners, T.; Schollmeyer, E. Permanent flame retardant finishing of textile materials by a photochemical immobilization of vinyl phosphonic acid. *Polym. Degrad. Stab.* **2011**, *96*, 393–395. [CrossRef]
28. Tsafack, M.J.; Levalois-Grützmacher, J. Flame retardancy of cotton textiles by plasma-induced graft-polymerization (PIGP). *Surf. Coat. Technol.* **2006**, *201*, 2599–2610. [CrossRef]
29. Totolin, V.; Sarmadi, M.; Manolache, S.O.; Denes, F.S. Atmospheric pressure plasma enhanced synthesis of flame retardant cellulosic materials. *J. Appl. Polym. Sci.* **2010**, *117*, 281–289. [CrossRef]

30. Brancatelli, G.; Colleoni, C.; Massafra, M.R.; Rosace, G. Effect of hybrid phosphorus-doped silica thin films produced by sol-gel method on the thermal behavior of cotton fabrics. *Polym. Degrad. Stab.* **2011**, *96*, 483–490. [CrossRef]
31. Alongi, J.; Ciobanu, M.; Malucelli, G. Sol–gel treatments on cotton fabrics for improving thermal and flame stability: Effect of the structure of the alkoxysilane precursor. *Carbohydr. Polym.* **2012**, *87*, 627–635. [CrossRef] [PubMed]
32. Alongi, J.; Ciobanu, M.; Malucelli, G. Thermal stability, flame retardancy and mechanical properties of cotton fabrics treated with inorganic coatings synthesized through sol–gel processes. *Carbohydr. Polym.* **2012**, *87*, 2093–2099. [CrossRef]
33. Alongi, J.; Colleoni, C.; Malucelli, G.; Rosace, G. Hybrid phosphorus-doped silica architectures derived from a multistep sol–gel process for improving thermal stability and flame retardancy of cotton fabrics. *Polym. Degrad. Stab.* **2012**, *97*, 1334–1344. [CrossRef]
34. Zhou, T.; He, X.; Guo, C.; Yu, J.; Lu, D.; Yang, Q. Synthesis of a novel flame retardant phosphorus/nitrogen/siloxane and its application on cotton fabrics. *Text. Res. J.* **2015**, *85*, 701–708. [CrossRef]
35. Mahltig, B.; Haufe, H.; Böttcher, H. Functionalisation of textiles by inorganic sol–gel coatings. *J. Mater. Chem.* **2005**, *15*, 4385–4398. [CrossRef]
36. Mahltig, B.; Böttcher, H.; Rauch, K.; Dieckmann, U.; Nitsche, R.; Fritz, T. Optimized UV protecting coatings by combination of organic and inorganic UV absorbers. *Thin Solid Film.* **2005**, *485*, 108–114. [CrossRef]
37. Mahltig, B.; Fiedler, D.; Böttcher, H. Antimicrobial Sol–Gel Coatings. *J. Sol-Gel Sci. Technol.* **2004**, *32*, 219–222. [CrossRef]
38. Xing, Y.; Ding, X. UV photo-stabilization of tetrabutyl titanate for aramid fibers via sol–gel surface modification. *J. Appl. Polym. Sci.* **2007**, *103*, 3113–3119. [CrossRef]
39. Xing, Y.; Yang, X.; Dai, J. Antimicrobial finishing of cotton textile based on water glass by sol–gel method. *J. Sol-Gel Sci. Technol.* **2007**, *43*, 187–192. [CrossRef]
40. Abidi, N.; Hequet, E.; Tarimala, S.; Dai, L.L. Cotton fabric surface modification for improved UV radiation protection using sol–gel process. *J. Appl. Polym. Sci.* **2007**, *104*, 111–117. [CrossRef]
41. Alongi, J.; Colleoni, C.; Rosace, G.; Malucelli, G. Sol–gel derived architectures for enhancing cotton flame retardancy: Effect of pure and phosphorus-doped silica phases. *Polym. Degrad. Stab.* **2014**, *99*, 92–98. [CrossRef]
42. Alongi, J.; Colleoni, C.; Rosace, G.; Malucelli, G. Phosphorus- and nitrogen-doped silica coatings for enhancing the flame retardancy of cotton: Synergisms or additive effects? *Polym. Degrad. Stab.* **2013**, *98*, 579–589. [CrossRef]
43. Fidalgo, A.; Ilharco, L.M. The defect structure of sol–gel-derived silica/polytetrahydrofuran hybrid films by FTIR. *J. Non-Cryst. Solids* **2001**, *283*, 144–154. [CrossRef]
44. Vasiliu, I.; Gartner, M.; Anastasescu, M.; Todan, L.; Predoana, L.; Elisa, M.; Negrila, C.; Ungureanu, F.; Logofatu, C.; Moldovan, A.; et al. Structural and optical properties of the SiO_2–P_2O_5 films obtained by sol–gel method. *Thin Solid Film.* **2007**, *515*, 6601–6605. [CrossRef]
45. Laoutid, F.; Bonnaud, L.; Alexandre, M.; Lopez-Cuesta, J.M.; Dubois, P. New prospects in flame retardant polymer materials: From fundamentals to nanocomposites. *Mater. Sci. Eng. R Rep.* **2009**, *63*, 100–125. [CrossRef]
46. Dobele, G.; Rossinskaja, G.; Telysheva, G.; Meier, D.; Faix, O. Cellulose dehydration and depolymerization reactions during pyrolysis in the presence of phosphoric acid. *J. Anal. Appl. Pyrolysis* **1999**, *49*, 307–317. [CrossRef]
47. Nowakowski, D.J.; Woodbridge, C.R.; Jones, J.M. Phosphorus catalysis in the pyrolysis behaviour of biomass. *J. Anal. Appl. Pyrolysis* **2008**, *83*, 197–204. [CrossRef]
48. Babushok, V.; Tsang, W. Inhibitor rankings for alkane combustion. *Combust. Flame* **2000**, *123*, 488–506. [CrossRef]
49. Alongi, J.; Ciobanu, M.; Malucelli, G. Sol–gel treatments for enhancing flame retardancy and thermal stability of cotton fabrics: Optimisation of the process and evaluation of the durability. *Cellulose* **2011**, *18*, 167–177. [CrossRef]
50. Cireli, A.; Onar, N.; Ebeoglugil, M.F.; Kayatekin, I.; Kutlu, B.; Culha, O.; Celik, E. Development of flame retardancy properties of new halogen-free phosphorous doped SiO_2 thin films on fabrics. *J. Appl. Polym. Sci.* **2007**, *105*, 3748–3756. [CrossRef]
51. Hribernik, S.; Smole, M.S.; Kleinschek, K.S.; Bele, M.; Jamnik, J.; Gaberscek, M. Flame retardant activity of SiO_2-coated regenerated cellulose fibres. *Polym. Degrad. Stab.* **2007**, *92*, 1957–1965. [CrossRef]